

# On the design of plug-in hybrid fuel cell and lithium battery propulsion systems for coastal ships

P. Wu and R.W.G. Bucknall

*Marine Research Group, Department of Mechanical Engineering, University College London, London WC1E 7JE, UK*

**ABSTRACT:** A plug-in hybrid propulsion system comprising of a proton exchange membrane fuel cell (PEMFC) and lithium battery capable of being recharged in port offers a promising low carbon propulsion system for small coastal ships, e.g. small container ships, tankers and ferries, which typically sail over short routes at modest speeds. PEMFC operate at high efficiency and emit no harmful emissions, but their poor transient performance necessitates the need for an energy storage system such as a lithium battery. A shore-to-ship electrical connection is needed to recharge the lithium battery from the grid so as to improve the propulsion system performance both environmentally and economically. Production of both H<sub>2</sub> and grid electricity have a carbon footprint. In this paper a two-layer optimisation based methodology is used for the design of plug-in hybrid fuel cell and lithium battery propulsion systems for coastal ships. Results from a case study suggest that the design of hybrid PEMFC and battery propulsion systems should be influenced by the ‘well-to-propeller’ carbon footprint.

**KEYWORDS:** Plug-in hybrid fuel cell; energy storage system; hydrogen; ferry; propulsion system design.

## 1 INTRODUCTION

### 1.1 Fuel cells

Fuel cells offer the desirable combination of high efficiency and environmentally benign operation (Sharaf & Orhan 2014). Among the main fuel cell types, the low-temperature Proton Exchange Membrane Fuel Cell (PEMFC) and high-temperature fuel cells (e.g. solid oxide fuel cell and molten carbonate fuel cell) offer the most promising power sources for future marine propulsion applications (Luckose et al. 2009). However, the economic feasibility of fuel cells is currently compromised by their high cost, poor transient performance, poor reliability, availability of alternative fuel supplies e.g. H<sub>2</sub> and associated fuel bunkering facilities (de-Troya et al. 2016).

High-temperature fuel cells offer higher efficiency when compared to the PEMFC (van Biert et al. 2016). A higher operating temperature makes it possible to recover heat from the exhaust gas so as to improve overall thermal efficiency, e.g. a combined cycle plant. Importantly high-temperature fuel cells can use a range of fuel types including natural gas. However, the main challenges of high-temperature fuel cells in marine applications are their low overall power to

volume density, long start-up times, limited cycling times and transient performance (Welaya et al. 2011).

PEMFC have been successfully applied to a range of propulsion applications, e.g. road vehicles, submarines and inland water boats (Sasank et al. 2016, Pei & Chen 2014, Han et al. 2012). PEMFC offer improved power to volume density but their efficiency is lower than high-temperature fuel cells and they can only operate on H<sub>2</sub> (van Biert et al. 2016). Unlike natural gas, H<sub>2</sub> does not exist naturally on earth so is produced using various means including electrolysis and reformation of hydrocarbon fuels. Therefore, H<sub>2</sub> through life Global Warming Potential (GWP), production cost, bunkering and onboard storage will all influence the feasibility of using PEMFC in ships.

For coastal ships operating on short routes at modest speeds then PEMFC with their better power to volume ratio appear to be more suitable. The PEMFC is well developed and its price is falling (DOE 2015). PEMFC with lithium batteries will provide acceptable transient performance. The low volumetric energy density of the hydrogen fuel suggests efficient operation is required to minimise onboard storage facilities. The production of H<sub>2</sub> has a carbon footprint as does grid electricity production. This paper explores these factors for a low carbon propulsion system.

## NOMENCLATURE

### Acronyms

AC	Alternating current
DC	Direct current
EMS	Energy management strategy
ESS	Energy storage system
GWP	Global warming potential
HHV	High heating value
MOO	Multi-objective optimisation
NGSR	Natural gas steam reforming
PEMFC	Proton exchange membrane fuel cell
PIHFCB	Plug-in hybrid fuel cell and battery
SOC	State of charge

### Roman symbols

$C$	Lithium battery C-rate
$c_{eq}$	Equality constraint
$F_1$	Multi-objective optimisation 1 <sup>st</sup> objective function
$F_2$	Multi-objective optimisation 2 <sup>nd</sup> objective function
$f$	Single-objective optimisation objective function
$g_{fc}$	Fuel cell specific hydrogen consumption function
$J$	Time step number when the ship calls at the port
$K$	Total time step number
$L_{fc}$	Fuel cell lifetime, h
$L_{ESS}$	Lithium battery lifetime, h
$M_1$	Multi-objective optimisation 1 <sup>st</sup> constraint function
$M_2$	Multi-objective optimisation 2 <sup>nd</sup> constraint function
$P_{ESS}$	ESS power, kW
$P_{shore}$	Shore power, kW
$P_l$	Load power, kW
$P_{fc}^R$	Fuel cell rated power, kW
$P_{fc}$	Fuel cell power, kW

$P_{ESS}^R$	Lithium battery rated power, kW
$p_h$	H <sub>2</sub> price, \$/kg
$p_{fc}$	PEMFC price, \$/kW
$p_{ESS}$	Lithium battery ESS price, \$/kWh
$p_e$	Shore electricity price, \$/kWh
$R_{fc}$	Fuel cell power ramp up/down limit
$SOC_i$	Lithium battery state of charge at $i$ -th time step
$T$	Voyage time, h
$\Delta t$	Time step length, h
$V_D$	Equivalent diesel system total volume, m <sup>3</sup>
$V_{df}$	Diesel fuel tank volume, m <sup>3</sup>
$W_D$	Equivalent diesel system total weight, t
$w_h$	H <sub>2</sub> specific GWP, kg CO <sub>2</sub> /kg
$w_e$	Electricity specific GWP, kg CO <sub>2</sub> /kWh
$x$	Decision vector
$x_{1,2,\dots,K}$	PEMFC stack per unit power output
$x_{K+1,K+2,\dots,2K}$	Lithium battery C-rate

### Greek symbols

$\rho_{fc}^v$	PEMFC stack volumetric power density, kW/m <sup>3</sup>
$\rho_{ESS}^v$	ESS stack volumetric energy density, kWh/m <sup>3</sup>
$\rho_t^v$	H <sub>2</sub> tank volumetric energy density, m <sup>3</sup> /kg H <sub>2</sub>
$\rho_{dg}^v$	Diesel engine volumetric power density, kW/t
$\rho_{fc}^g$	PEMFC stack gravimetric power density, kW/t
$\rho_{ESS}^g$	ESS gravimetric energy density, kWh/t
$\rho_t^g$	H <sub>2</sub> tank gravimetric energy density, kg/kg H <sub>2</sub>
$\eta_1$	Uni-directional converter efficiency
$\eta_2$	Bi-directional converter efficiency
$\eta_b$	Lithium battery efficiency

## 1.2 Energy storage systems

Energy Storage Systems (ESS) such as lithium batteries have already been adopted for use in commercial ship applications, often in a configuration of hybridisation with the diesel engine (Luo et al. 2015). When hybrid configurations are used, they can potentially achieve 15% annual fuel saving depending on operational profile, e.g. the Viking Lady offshore supply vessel (Stefanatos et al. 2015). When only a battery is used alone for propulsion, e.g. the Norled Ampere battery powered ferry, then the low volumetric energy density of the batteries restricts both speed and range.

For a marine Plug-in Hybrid Fuel Cell Battery (PIHFCB) propulsion system, the ESS provides transient capability and greater plant efficiency. Furthermore, when a shore charging facility is available, integration of ESS can further improve the overall energy efficiency through direct utilisation of clean grid electricity e.g. electrolysis of water generating H<sub>2</sub> rather than reformation of hydrocarbon fuels. For a PIHFCB propulsion system, lithium batteries are

preferable over other main ESS types for better energy density (Hannan et al. 2017).

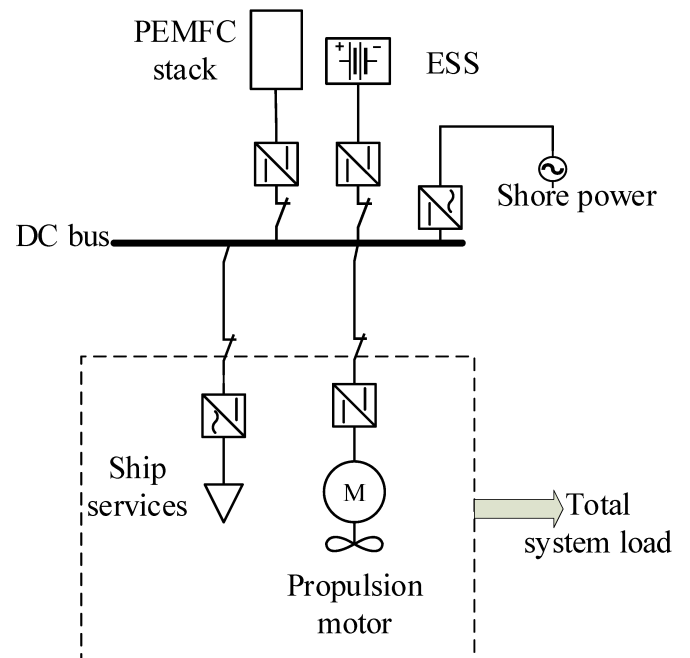


Figure 1. PIHFCB propulsion system layout.

### 1.3 Design methodology

Using fuel cells and batteries together the overall GWP can potentially be very low or even zero when renewable energy is utilised for electricity generation and hydrogen (Hansen & Wendt 2015). There are some research studies, e.g. Bassam et al. (2016) and Mashayekh et al. (2012) who have looked into the optimisation of hybrid ship propulsion systems. These works only focus on cost optimisation without considering the overall environmental performance of the propulsion plant i.e. well-to-propeller.

When multiple power sources are integrated into one propulsion system, two problems need to be resolved: 1) How to size the different energy and power sources to achieve an optimised well-to-propeller emission performance; 2) How to manage the different power sources to maintain high overall efficiency.

Since this paper is considering a PIHFCB propulsion system suitable for coastal ships which typically sail on short routes at modest speeds the analysis needs to consider GWP emissions and operating costs. The propulsion system design methodology consists two layers of optimisation:

1. An external layer applies a controlled elitist Multi-Objective Optimisation (MOO) scheme using evolutionary algorithms to optimise environmental and economic performance thereby overcoming the constraints on the propulsion plant design such as volumetric and gravimetric limits of the ESS and H<sub>2</sub> (Deb 2001).
2. The inner layer optimisation scheme utilises dynamic programming to generate most optimal Energy Management Strategy (EMS) for multiple power sources knowing the powering requirements and the operating profile.

## 2 PLUG-IN HYBRID PEMFC AND ESS PROPULSION SYSTEM

### 2.1 Basic concept of operation

There are different operating modes for coastal ships which need to be considered independently:

When the ship is at sea, both the PEMFC stack and lithium batteries work concurrently to power the ship propulsion and its service loads. The ESS has two functions: 1) Levelling the PEMFC stack loads to achieve the best overall efficiency; 2) Utilising the stored clean grid power to achieve the best overall environmental performance.

When the ship is manoeuvring, then the battery should supplement the fuel cell set at a lower output. The battery will charge or discharge as needed to reduce transients to the fuel cell but also to maintain high overall efficiency.

When the ship is in port, shore power is available to charge the ESS and to power the ship's services, i.e. cold ironing.

Due to the high volumetric demands of H<sub>2</sub> fuel it is assumed that the ship bunkers H<sub>2</sub> fuel for each voyage, i.e. every time it calls at the port.

### 2.2 System layout

Figure 1 presents the PIHFCB propulsion system layout. DC power distribution architecture is preferred since the power out from both PEMFC stack, and ESS is DC electrical power (Zahedi et al. 2014).

### 2.3 Propulsion system dynamics

According to energy conservation principle, the relationship between the PEMFC stack output power  $P_{fc}$ , battery power  $P_{ESS}$ , shore power  $P_{shore}$  and the lumped system power demand  $P_l$  can be determined as:

$$P_{fc}\eta_1 + P_{ESS}\eta_2\eta_b + P_{shore}\eta_1 - P_l = 0 \quad (1)$$

where  $\eta_1$ ,  $\eta_2$  and  $\eta_b$  are uni-directional, bi-directional converter efficiency and lithium battery ESS efficiency respectively; and  $P_{shore} = 0$  when ship is sailing,  $P_{shore} \geq 0$  when ship is at port.  $P_{ESS} > 0$  when lithium battery ESS discharges, and  $P_{ESS} < 0$  while ESS charges.

### 2.4 Proton exchange membrane fuel cell

The PEMFC stack model is developed and calibrated using the methodology and data from (Larminie et al. 2003), (Tremblay & Dessaint 2009) and (Li et al. 2009). The PEMFC model is simplified to represent per unit power versus specific H<sub>2</sub> consumption based on the 141.8 MJ/kg H<sub>2</sub> High Heating Value (HHV) as presented in Figure 2 (Koroneos et al. 2004). The PEMFC stack specific H<sub>2</sub> consumption is given by:

$$SHC = g_{fc}(x) \quad (2)$$

where  $SHC$  is the specific H<sub>2</sub> consumption and is a function  $g_{fc}$  of the PEMFC stack per unit power  $x$ ,  $0 \leq x \leq 1$ . For the rated PEMFC stack power of  $P_{fc}^R$ , the power output from the PEMFC stack is:

$$P_{fc} = P_{fc}^R x \quad (3)$$

### 2.5 Energy storage system

As lithium battery features high efficiency for charging and discharging, the round-trip efficiency of ESS charging/discharging is assumed as  $\eta_b = 0.98$  within allowed State of Charge (SOC) range, e.g.  $0.2 \leq SOC \leq 1$  (Ovrum & Bergh 2015). The SOC range is set to avoid excessive degradation due to

over-discharge. Note that, the initial SOC is one. At time step  $t$ , SOC is calculated by:

$$SOC = 1 - \int_0^t C(t)dt \quad (4)$$

where  $C(t)$  is ESS charge/discharge C-rate at time step  $t$ . And  $P_{ESS} = C(t)P_{ESS}^R$ , where  $P_{ESS}^R$  is ESS power when C-rate is 1.

### 2.6 Power converters

Figure 3 shows the power converter efficiency characteristics used in this study (Martel et al. 2015). The uni-directional efficiency is slightly higher than that of a bi-directional one.

## 3 HYBRID SYSTEM DESIGN METHODOLOGY

Ship power and propulsion systems are customised for individual ships to provide efficient and reliable operation. The design of hybrid propulsion systems comprising multiple power sources should be optimised for the specific operational requirements and scenarios to exploit merits and avoid drawbacks of each type of power sources effectively. The electricity and alternative fuels (e.g. H<sub>2</sub>) characteristics can vary from place to place. Also, novel power technologies such as fuel cells and batteries are typically limited by high production costs, limited lifetime and power/energy density for marine propulsion systems. These factors need to be considered for propulsion system designs.

### 3.1 Methodology overview

The proposed design methodology includes two layers of optimisation schemes as presented in Figure 4. The external MOO scheme searches predefined ranges to find optimum PEMFC stack rated power, ESS capacity and shore charging power. The power and propulsion solutions need to meet both volumetric and gravimetric constraints on the propulsion plant. The inner optimisation scheme based on dynamic programming determines the EMS for each combination of power sources generated by the external layer. The EMS minimises the voyage fuel costs satisfying the powering demands and power sources constraints.

### 3.2 Multi-objective genetic algorithm – sizing optimisation

The MOO solutions, in the form of Pareto fronts, allow the decision makers to make informed decisions by seeing a set of acceptable trade-off optimal solutions (Ngatchou et al. 2005). In this case, the trade-offs are between equivalent voyage GWP and average voyage cost. The former includes the equivalent CO<sub>2</sub>

emission throughout the lifecycle of H<sub>2</sub> and electricity. The average voyage cost consists of H<sub>2</sub> cost, electricity cost and PEMFC and ESS degradation costs.

#### 3.2.1 Decision variables

The decision variables of the external optimisation layer are rated PEMFC stack power  $P_{fc}^R$ , ESS capacity  $C_{ESS}^R$  and shore charging power  $P_{shore}^R$ . The searching range of the three variables are set considering the maximum power and total energy demands in operating profile as following:

$$P_{fc}^{min} \leq P_{fc}^R \leq P_{fc}^{max} \quad (5)$$

$$C_{ESS}^{min} \leq C_{ESS}^R \leq C_{ESS}^{max} \quad (6)$$

$$P_{shore}^{min} \leq P_{shore}^R \leq P_{shore}^{max} \quad (7)$$

#### 3.2.2 Objective functions

The first objective function of MOO is the average voyage cost, which includes H<sub>2</sub> fuel and electricity cost for one voyage, battery and PEMFC stack degradation costs for one voyage:

$$F_1 = \sum_{i=1}^K g_{fc}(x_i) x_i P_{fc}^R \Delta t p_h + \sum_{i=J}^K P_{shore}^R \Delta t (K - J) p_e + \left( \frac{p_{fc} P_{fc}^R}{L_{fc}} + \frac{p_{ESS} C_{ESS}^R}{L_{ESS}} \right) \quad (8)$$

where  $p_h$  is the H<sub>2</sub> price in \$/kg,  $p_{fc}$  is the PEMFC stack price in \$/kW,  $p_{ESS}$  is the battery price in \$/kWh,  $K$  is the total time step number,  $i$  is  $i$ -th time step,  $J$  is the time step number when the ship calls at the port,  $T$  is the voyage time,  $\Delta t = T/K$  is time step length,  $L_{fc}$  and  $L_{ESS}$  are fuel cell and battery lifetime respectively.

The second objective function of MOO is the GWP emission for one voyage, which is the sum of H<sub>2</sub> fuel GWP and shore electricity GWP in equivalent kg CO<sub>2</sub>:

$$F_2 = \sum_{i=1}^K g_{fc}(x_i) x_i P_{fc}^R \Delta t w_h + P_{shore}^R \Delta t (K - J) w_e \quad (9)$$

where  $w_h$  and  $w_e$  are H<sub>2</sub> and electricity specific GWP respectively.

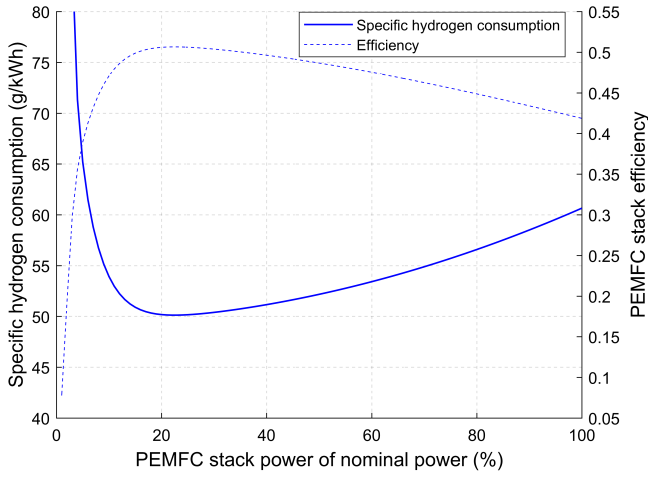


Figure 2. PEMFC stack specific H<sub>2</sub> consumption and efficiency.

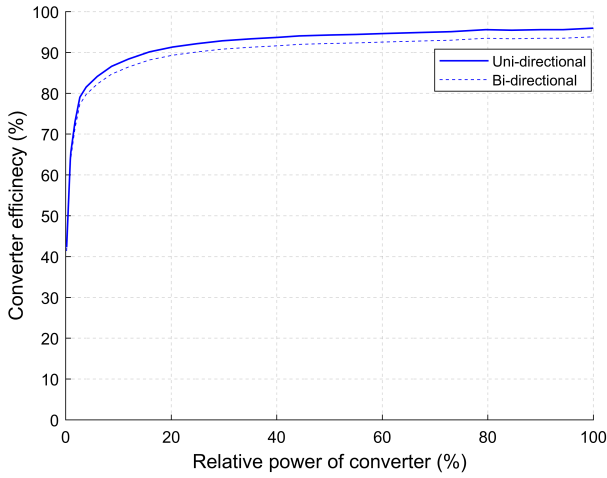


Figure 3. Power electronics characteristics.

### 3.2.3 Constraints

The first constraint function limits the hybrid propulsion system volume does not exceed the equivalent diesel-mechanical system volume. The difference between the hybrid propulsion system and the diesel-mechanical plant is:

$$M_1 = P_{fc}^R \rho_{fc}^v + C_{ESS}^R \rho_{ESS}^v + \sum_{i=1}^K g_{fc}(x_i) x_i P_{fc}^R \Delta t \rho_t^v - V_D \leq 0 \quad (10)$$

where  $\rho_{fc}^v$ ,  $\rho_{ESS}^v$  and  $\rho_t^v$  are volumetric density of PEMFC stack, ESS and H<sub>2</sub> tank (contains H<sub>2</sub> for one voyage) respectively,  $V_D$  is the equivalent diesel system total volume and  $V_D = P_{dg} \rho_{dg}^v + V_{df}$ ,  $\rho_{dg}^v$  is the diesel engine volumetric power density, and  $V_{df}$  is the diesel fuel tank volume. It is assumed the original case ship refuels diesel once a week in the subsequent analysis.

The second constraint function limits the hybrid propulsion system total weight does not exceed the equivalent diesel-mechanical system weight:

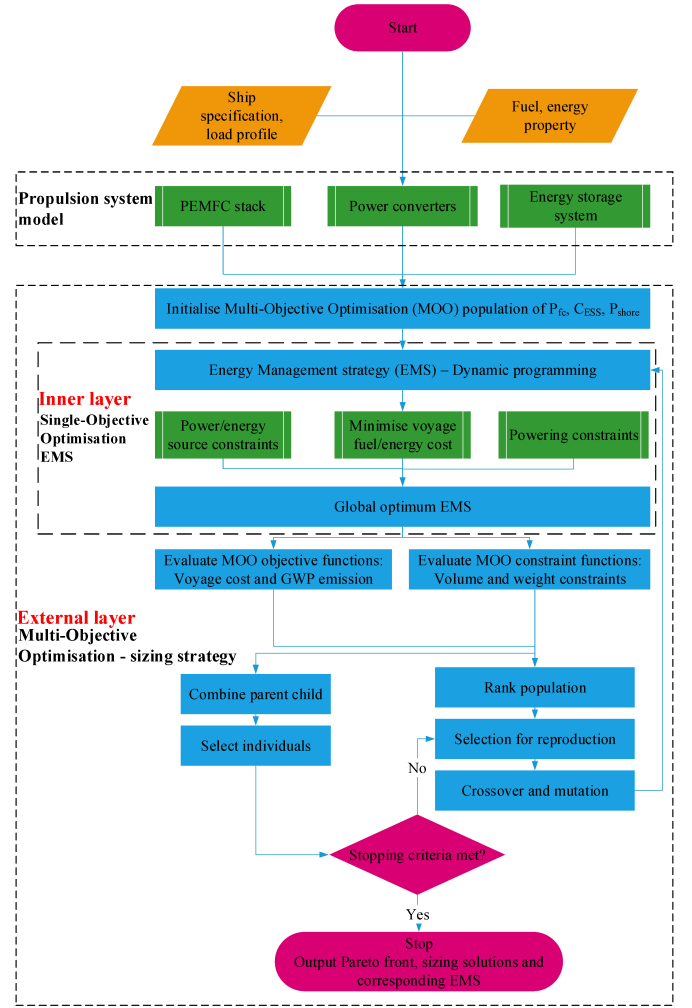


Figure 4. Hybrid system design methodology.

$$M_2 = P_{fc}^R \rho_{fc}^g + C_{ESS}^R \rho_{ESS}^g + \sum_{i=1}^K g_{fc}(x_i) x_i P_{fc}^R \Delta t (\rho_t^g + 1) - W_D \leq 0 \quad (11)$$

where  $\rho_{fc}^g$ ,  $\rho_{ESS}^g$ , and  $\rho_t^g$  are the gravimetric density of PEMFC stack, battery and H<sub>2</sub> tank respectively,  $W_D$  is the diesel based system total weight including the diesel engine, gearbox and fuel weight.

### 3.3 Dynamic programming – Energy Management Strategy solving

The inner optimisation scheme applies dynamic programming based on Bellman's optimality principle to find the most optimal EMS with load profile is known before solving (Bellman 2013). The dynamic programming approach can be used to find the optimal EMS which can be used as a benchmark to evaluate the effectiveness of on-line real-time EMS (Song et al. 2014). The EMS solution for each power and energy source combination is passed to external MOO to evaluate the objective and constraint functions. The

objective function values of MOO are infinite if no EMS solution exists.

### 3.3.1 Decision variables

The decision variables represent specific loading conditions for PEMFC stack and ESS. The shore connection delivers rated power whenever the ship is in port. The decision vector is:

$$x = [x_1, x_2, \dots, x_K | x_{K+1}, x_{K+2}, \dots, x_{2K}] \quad (12)$$

where  $x_1, x_2, \dots, x_K$  are per unit power of the PEMFC stack, and  $x_{K+1}, x_{K+2}, \dots, x_{2K}$  are the C-rate of the ESS from 1<sup>st</sup> to K<sup>th</sup> (final step of one voyage) time step.

### 3.3.2 Objective functions

The objective function of the inner optimisation scheme is the voyage total fuel and electricity cost:

$$f = \sum_{i=1}^K g_{fc}(x_i) x_i P_{fc}^R p_h + P_{shore}^R \Delta t (K - J) p_e \quad (13)$$

### 3.3.3 Constraints

#### 3.3.3.1 Powering

For each time step, the power provided by all the power and energy sources should equal to the sum of load demand and system losses, therefore re-write Eq. (1) to discrete form:

$$c_{eq,i} = x_i P_{fc}^R \eta_1(x_i) + x_{i+K} P_{ESS}^R \eta_2(x_{i+K}) \eta_b + P_{shore} \eta_1(1) - P_{l,i} = 0 \quad (14)$$

#### 3.3.3.2 ESS state of charge

The battery SOC needs to be within a range to avoid over-charge or over-discharge, therefore:

$$SOC_{min} \leq SOC_i \leq SOC_{max} \quad (15)$$

moreover:

$$SOC(i) = 1 - \sum_1^i x_{K+i} dt \quad (16)$$

#### 3.3.3.3 Fuel cell power ramp up/down rates

Compared to diesel engines, PEMFC stack is weak in transient loads. Therefore, the fuel cell power change between two adjacent time steps should satisfy:

$$|x_i - x_{i-1}| \leq R_{fc} \quad (17)$$

where  $R_{fc}$  is the fuel cell power ramp up/down limit.

## 4 CASE STUDY

### 4.1 Case ship specification

In the case study, the proposed methodology is applied to design the PIHFCB propulsion system considering both environmental and economic performance for case ship which sails on short routes. The vessel specification is shown in Table 1 (Traffic 2015).

### 4.2 Case ship operating profile

For system level design and optimisation, the load profile of the case ship is modelled as a lumped power profile including both propulsion and service loads as shown in Figure 5 (Mashayekh et al. 2012). The load ramps up to a high value in the first 10 minutes and fluctuates to follow a sinusoidal wave to mock the power demand variations. Then the ship power ramps down (90-100 mins) to the port where shore connection charges the battery if necessary. Shore power is available to charge from 100 to 140 mins. This system load profile is converted into a discrete time series and repeats for each voyage.

Table 2 presents the price and specific GWP of H<sub>2</sub> generated via three typical approaches (Acar & Dincer 2014). The three types of H<sub>2</sub> were analysed to investigate the impacts from H<sub>2</sub> properties to the design of propulsion system. The electricity price is assumed to be \$0.12/kWh, and its GWP is 0.289 kg/kWh (Eurostat 2017).

### 4.3 Case study parameters

Table 3 describes the parameters applied in the case study. The PEMFC stack and battery properties, the prices are all for system level, i.e. including the ancillary devices. It worth mentioning that the results are sensitive to the parameters.

### 4.4 Sizing results

#### 4.4.1 Pareto fronts

Table 1. Case ship specification (Traffic 2015).

Vessel type	Ro-ro/passenger ship	
Gross tonnage	3,193 tons	
Deadweight	572 tons	
Length overall	87 m	
Breadth extreme	17 m	
Designed speed	12 knots	
Installed engine power	2,148 kW	

Table 2. H<sub>2</sub> characteristics (Acar & Dincer 2014).

H <sub>2</sub> generation method	Price (\$/kg)	GWP (kg CO <sub>2</sub> /kg)
Nuclear Cu-Cl	1.7	1.6
Wind	7.2	1.3
Natural gas steam reforming (NGSR)	1.5	7.5

Table 3. Case study parameters.

Parameters	Value	Reference
Annual operating days	300 days	(Traffic 2015)
Daily voyage number	6	(Traffic 2015)
Fuel cell price	\$1200/kWh	(Isa et al. 2016)
Fuel cell lifetime	3 years (or 10,800 h)	(Ballard 2017)
Battery price	\$800/kWh	(Ovrum & Bergh 2015)
Battery lifetime	3 years	(Stroe et al. 2015)
Shore electricity price	\$0.12/kWh	(Eurostat 2017)
Shore electricity GWP	0.289 kg CO <sub>2</sub> /kWh	(Eurostat 2017)
PEMFC volumetric specific power	128.2 kW/m <sup>3</sup>	(Ballard 2017)
PEMFC gravimetric specific power	200.0 kW/t	(Ballard 2017)
ESS volumetric specific energy	91.8 kWh/m <sup>3</sup>	(Corvus 2017)
ESS gravimetric specific energy	80.6 kWh/t	(Corvus 2017)
Battery maximum C-rate	6.0	(Corvus 2017)
Diesel engine volumetric specific power	43.9 kW/m <sup>3</sup>	(Wartsila 2016)
Diesel engine with gearbox specific power	54.8 kW/t	(Wartsila 2016)
Marine gas oil price	\$0.64/kg	(BunkerIndex 2017)
H <sub>2</sub> tank volume	0.17 m <sup>3</sup> /kg H <sub>2</sub>	(Choi et al. 2016)
H <sub>2</sub> tank weight	28.5 kg/kg H <sub>2</sub>	(Choi et al. 2016)

Figure 6 shows the Pareto fronts for H<sub>2</sub> produced from the three sources mentioned in Table 2. For the case of H<sub>2</sub> generated via Nuclear Cu-Cl, as both the H<sub>2</sub> specific GWP and price low, the Pareto front points only distribute in a small region of shore power. H<sub>2</sub> generated using wind power features for the lowest GWP, but the highest price can achieve best emission performance but leads to high voyage costs. The Pareto front of NGSR H<sub>2</sub> can contribute the lowest average cost, but also the highest GWP. In general, Nuclear Cu-Cl generated H<sub>2</sub> excels the other two.

#### 4.4.2 Optimal sizing

Figure 7 presents the detailed Pareto front solutions including the information of PEMFC stack rated power, battery capacity and rated shore power. The optimal shore power distributed between a narrow region from 180 to 185 kW, which is because both the H<sub>2</sub> specific GWP and price are low amongst the three H<sub>2</sub> production methods. Furthermore, increasing the average voyage cost cannot further improve emission performance effectively. ESS mainly functions as an energy buffer to optimise PEMFC stack loading to achieve higher efficiency.

For the wind power generated H<sub>2</sub> case, as presented in Figure 8, the optimal solutions scatter in more substantial space. The combinations with high shore charging power and larger ESS capacity correspond to better emission performance (Figure 8b), but worse economic feasibility (Figure 8a). Such trends match the wind power generated H<sub>2</sub> property – high price, but low specific GWP.

In contrast, Figure 9 shows the trade-off between economic and environmental performances for the H<sub>2</sub> generated via NGSR (high specific GWP and low

price). Higher PEMFC stack power leads to lower running cost (Figure 9a) but higher GWP (Figure 9b).

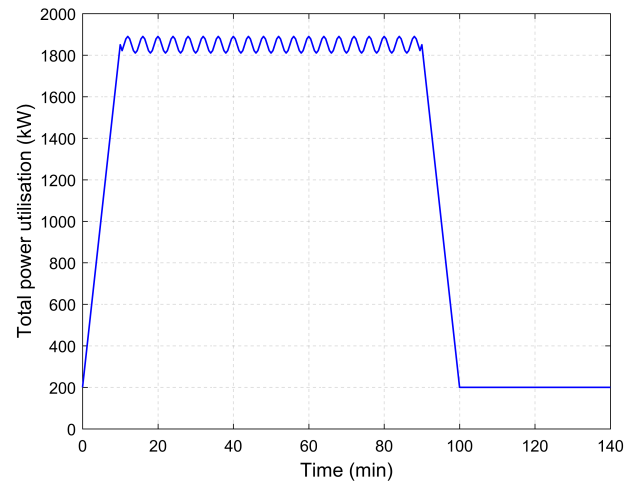


Figure 5. Case ship lumped load profile.

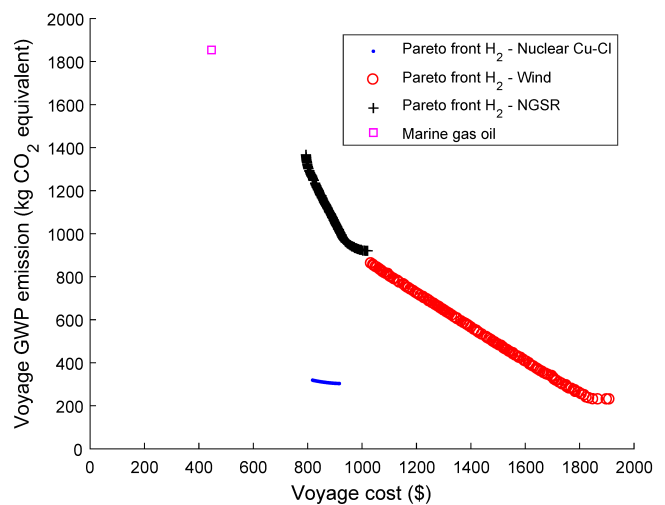


Figure 6. Pareto fronts.

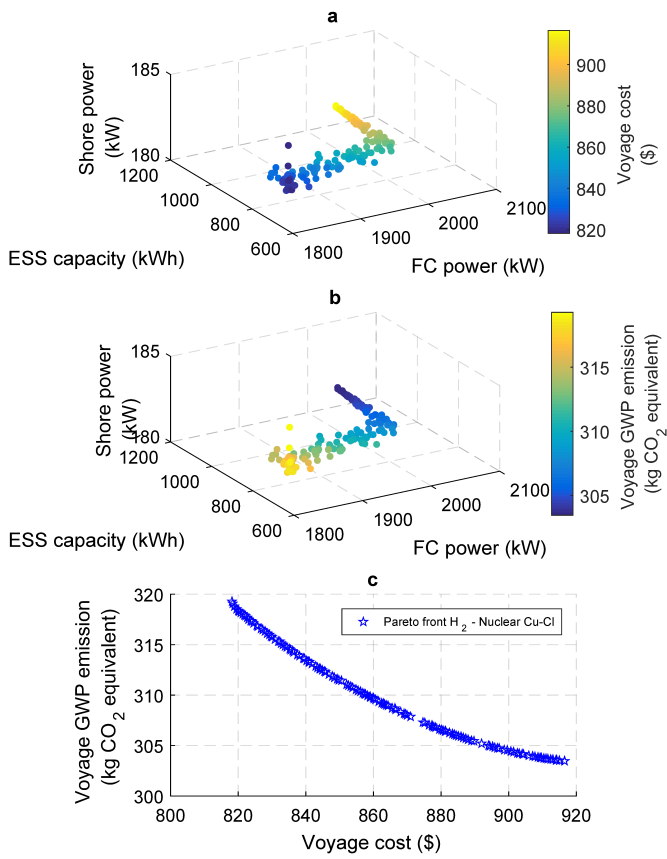


Figure 7. Power source sizing results of H<sub>2</sub> generated via Nuclear Cu-Cl method: (a) average voyage cost, (b) voyage GWP and (c) Pareto front.

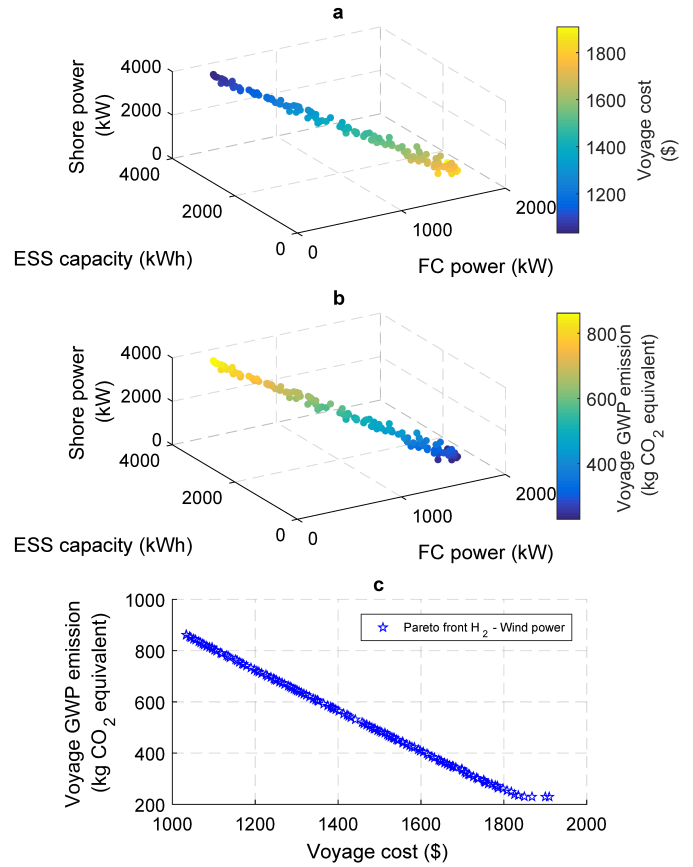


Figure 8. Power source sizing results of H<sub>2</sub> generated via wind power: (a) average voyage cost, (b) voyage GWP and (c) Pareto front.

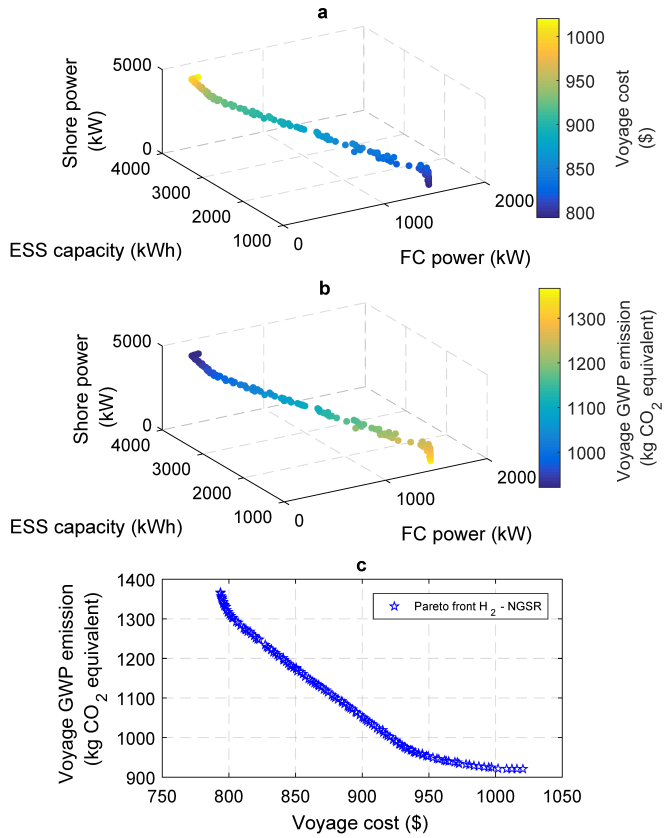


Figure 9. Power source sizing results of H<sub>2</sub> generated via NGRS: (a) average voyage cost, (b) voyage GWP and (c) Pareto front.

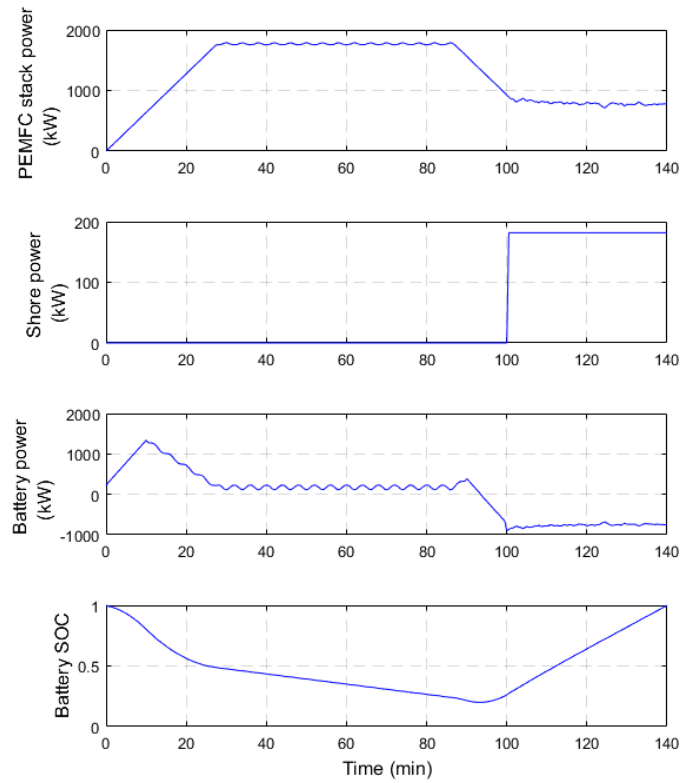


Figure 10. EMS of Nuclear Cu-Cl generated H<sub>2</sub> sample case: ESS capacity – 692 kWh, PEMFC stack power – 1823 kW and shore power – 182 kW.



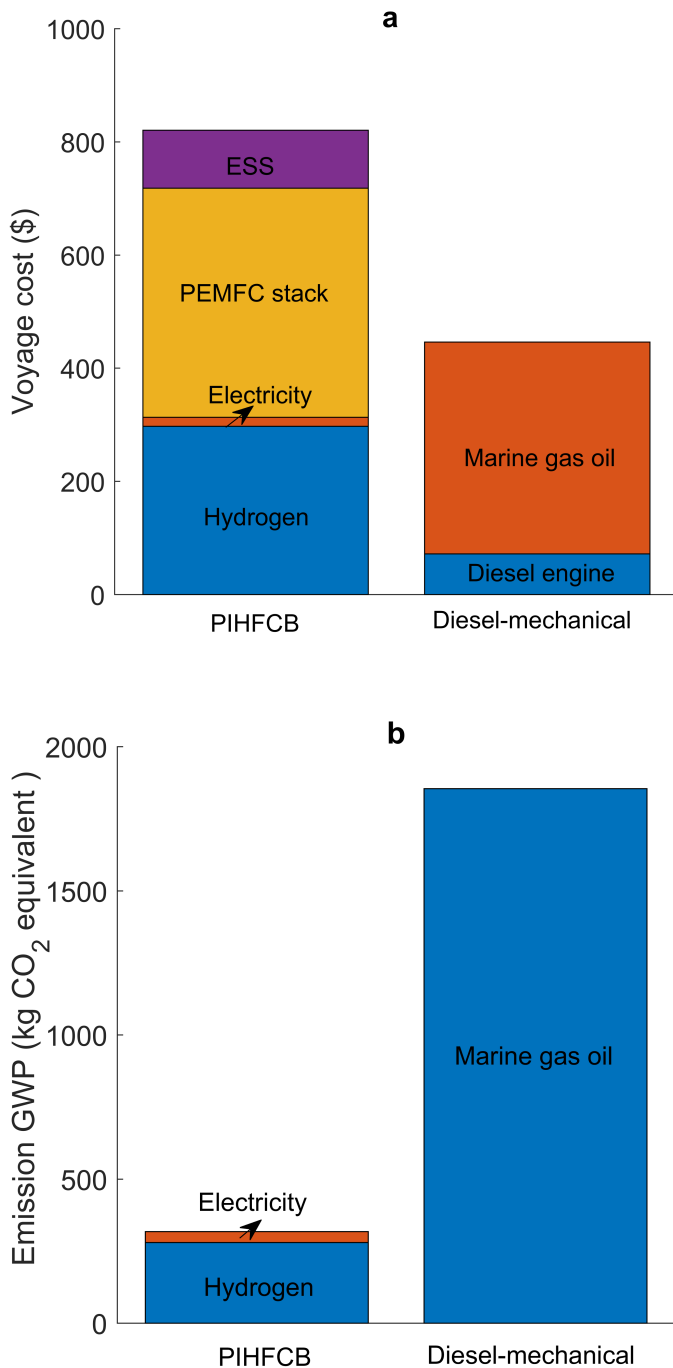


Figure 11. Voyage cost (a) and voyage GWP (b) breakdown comparison of Nuclear Cu-Cl generated H<sub>2</sub> sample case: ESS capacity – 692 kWh, PEMFC stack power – 1823 kW and shore power – 182 kW vs baseline diesel-mechanical system.

Figure 10 presents the most optimal EMS for H<sub>2</sub> generated by Nuclear Cu-Cl case: the ESS capacity is 692 kWh, PEMFC stack power is 1823 kW, and shore power is 182 kW. The battery starts to provide most of the power demands at the beginning while the PEMFC stack increases the power output gradually and takes over most of the load. The battery tackles most of the power transients during cruising. It is interesting that when the ship is at the port, the fuel cell stack still delivers power to the system, which is mainly due to the H<sub>2</sub> generated by Nuclear Cu-Cl is cheap.

Figure 11 compares the voyage cost and GWP emission breakdown between diesel-mechanical plant operating on marine gas oil and the alternative PIHFBC propulsion system (the scenario discussed in Figure 10). The average voyage cost of the hybrid system is approximately 70% higher than the diesel-mechanical system. Nevertheless, about 60% of the hybrid system voyage cost is from battery and PEMFC stack degradation. The fuel cell and battery technologies have been evolving rapidly in the past decade, which can potentially cut down the cost significantly (Sharaf & Orhan 2014, Nykvist & Nilsson 2015).

## 5 CONCLUSIONS

This paper presents a PIHFBC design methodology for coastal ships sail on short routes and have accessibility to H<sub>2</sub> bunkering and battery charging facilities. The two-layer optimisation methodology has been shown to generate optimal sizing solutions with an energy management strategy for each design point. Instead of providing a single design point, the solution space provides the decision makers with a better view of the trade-offs between overall emission reduction and commercial feasibility.

The case study results show that electricity and H<sub>2</sub> characteristics have a significant influence on the design of hybrid PEMFC and battery propulsion system. The volumetric and gravimetric impacts from H<sub>2</sub> fuel, PEMFC stack and battery can be mitigated for coastal ships sail on short routes with easy access to H<sub>2</sub> bunkering and battery charging facilities. Fuel cell and battery degradation can potentially contribute to more than 50% of the average voyage cost, while marine gas oil is the main portion for that of a diesel-mechanical plant. Fuel cell and battery lifetime and durability are expected to be improved to be commercially competitive with conventional diesel engine based propulsion plants. Nevertheless, the GWP emission reduction from the PIHFBC propulsion system can be more than 25%, even using H<sub>2</sub> produced from NGRS.

As the degradation of both PEMFC and battery could potentially impact the average voyage cost significantly, more detailed PEMFC and battery degradation models are expected to be included in future work.

## ACKNOWLEDGEMENTS

The first author would like to thank the China Scholarship Council (CSC) and University College London for supporting his studies at University College London, UK.

## REFERENCES

- Acar, C. & Dincer, I. 2014. Comparative assessment of hydrogen production methods from renewable and non-renewable sources. *International Journal of Hydrogen Energy*, 39(1), 1-12.
- Ballard, 2017. *Key Advantages of Ballard's Fuel Cell Stack Products* [online]. Available from: <http://www.ballard.com/fuel-cell-solutions/fuel-cell-power-products/fuel-cell-stacks> [Accessed 10th/Oct 2017].
- Bassam, A. M., Phillips, A. B., Turnock, S. R. & Wilson, P. A., Sizing optimization of a fuel cell/battery hybrid system for a domestic ferry using a whole ship system simulator. In: *2016 International Conference on Electrical Systems for Aircraft, Railway, Ship Propulsion and Road Vehicles & International Transportation Electrification Conference (ESARS-ITEC)*, 2-4 Nov. 2016 2016, 1-6.
- Bellman, R., 2013. *Dynamic programming*. Courier Corporation.
- BunkerIndex, 2017. *Index Summary* [online]. Available from: <http://www.bunkerindex.com/> [Accessed 28th/10 2015].
- Choi, C. H., Yu, S., Han, I.-S., Kho, B.-K., Kang, D.-G., Lee, H. Y., . . . Kim, M. 2016. Development and demonstration of PEM fuel-cell-battery hybrid system for propulsion of tourist boat. *International Journal of Hydrogen Energy*, 41(5), 3591-3599.
- Corvus, E., 2017. *Orca Energy Specifications* [online]. Available from: <http://corvusenergy.com/technology-specifications/> [Accessed 10th/Oct 2017].
- de-Troya, J. J., Álvarez, C., Fernández-Garrido, C. & Carral, L. 2016. Analysing the possibilities of using fuel cells in ships. *International Journal of Hydrogen Energy*, 41(4), 2853-2866.
- Deb, K., 2001. *Multi-objective optimization using evolutionary algorithms*. John Wiley & Sons.
- DOE, 2015. *Fuel cell technologies office accomplishments and progress* [online]. Available from: <http://energy.gov/eere/fuelcells/fuel-cell-technologies-office-accomplishments-and-progress> [Accessed 10th/Sep 2015].
- Eurostat, 2017. *Electricity price statistics* [online]. Available from: [http://ec.europa.eu/eurostat/statistics-explained/index.php/Electricity\\_price\\_statistics](http://ec.europa.eu/eurostat/statistics-explained/index.php/Electricity_price_statistics) [Accessed 10th/Dec 2017].
- Han, J., Charpentier, J. F. & Tianhao, T., State of the art of fuel cells for ship applications. In: *Industrial Electronics (ISIE), 2012 IEEE International Symposium on*, 28-31 May 2012 2012, 1456-1461.
- Hannan, M. A., Hoque, M. M., Mohamed, A. & Ayob, A. 2017. Review of energy storage systems for electric vehicle applications: Issues and challenges. *Renewable and Sustainable Energy Reviews*, 69, 771-789.
- Hansen, J. F. & Wendt, F. 2015. History and State of the Art in Commercial Electric Ship Propulsion, Integrated Power Systems, and Future Trends. *Proceedings of the IEEE*, 103(12), 2229-2242.
- Isa, N. M., Das, H. S., Tan, C. W., Yatim, A. H. M. & Lau, K. Y. 2016. A techno-economic assessment of a combined heat and power photovoltaic/fuel cell/battery energy system in Malaysia hospital. *Energy*, 112, 75-90.
- Koroneos, C., Dompros, A., Roumbas, G. & Moussiopoulos, N. 2004. Life cycle assessment of hydrogen fuel production processes. *International Journal of Hydrogen Energy*, 29(14), 1443-1450.
- Larminie, J., Dicks, A. & McDonald, M. S., 2003. *Fuel cell systems explained*. J. Wiley Chichester, UK.
- Li, X., Xu, L., Hua, J., Lin, X., Li, J. & Ouyang, M. 2009. Power management strategy for vehicular-applied hybrid fuel cell/battery power system. *Journal of Power Sources*, 191(2), 542-549.
- Luckose, L., Hess, H. L. & Johnson, B. K., Fuel cell propulsion system for marine applications. In: *2009 IEEE Electric Ship Technologies Symposium*, 20-22 April 2009 2009, 574-580.
- Luo, X., Wang, J., Dooner, M. & Clarke, J. 2015. Overview of current development in electrical energy storage technologies and the application potential in power system operation. *Applied Energy*, 137, 511-536.
- Martel, F., Kelouwani, S., Dubé, Y. & Agbossou, K. 2015. Optimal economy-based battery degradation management dynamics for fuel-cell plug-in hybrid electric vehicles. *Journal of Power Sources*, 274, 367-381.
- Mashayekh, S., Wang, Z., Qi, L., Lindtjorn, J. & Myklebust, T. A., Optimum sizing of energy storage for an electric ferry ship. In: *2012 IEEE Power and Energy Society General Meeting*, 22-26 July 2012 2012, 1-8.
- Ngatchou, P., Zarei, A. & El-Sharkawi, A., Pareto multi objective optimization. In: *Intelligent systems application to power systems, 2005. Proceedings of the 13th international conference on*, 2005, 84-91.
- Nykvist, B. & Nilsson, M. 2015. Rapidly falling costs of battery packs for electric vehicles. *Nature Clim. Change*, 5(4), 329-332.
- Ovrum, E. & Bergh, T. F. 2015. Modelling lithium-ion battery hybrid ship crane operation. *Applied Energy*, 152, 162-172.
- Pei, P. & Chen, H. 2014. Main factors affecting the lifetime of Proton Exchange Membrane fuel cells in vehicle applications: A review. *Applied Energy*, 125, 60-75.
- Sasank, B. V., Rajalakshmi, N. & Dhathathreyan, K. S. 2016. Performance analysis of polymer electrolyte membrane (PEM) fuel cell stack operated under marine environmental conditions. *Journal of Marine Science and Technology*, 1-8.
- Sharaf, O. Z. & Orhan, M. F. 2014. An overview of fuel cell technology: Fundamentals and applications. *Renewable and Sustainable Energy Reviews*, 32, 810-853.
- Song, Z., Hofmann, H., Li, J., Hou, J., Han, X. & Ouyang, M. 2014. Energy management strategies comparison for electric vehicles with hybrid energy storage system. *Applied Energy*, 134, 321-331.
- Stefanatos, I. C., Dimopoulos, G. G., Kakalis, N. M. P., Vartdal, B. & Ovrum, E., Modelling and simulation of hybrid-electric propulsion systems: the Viking Lady case. In: *12th International Marine Design Conference*, 2015 Tokyo, 161-178.
- Stroe, A. I., Swierczynski, M., Stroe, D. I. & Teodorescu, R., Performance model for high-power lithium titanate oxide batteries based on extended characterization tests. In: *2015 IEEE Energy Conversion Congress and Exposition (ECCE)*, 20-24 Sept. 2015 2015, 6191-6198.
- Traffic, M., 2015. *Marine Traffic* [online]. Available from: <http://www.marinetraffic.com/> [Accessed 10th/Jan 2016].
- Tremblay, O. & Dessaint, L.-A., A generic fuel cell model for the simulation of fuel cell vehicles. In: *Vehicle Power and Propulsion Conference, 2009. VPPC'09. IEEE*, 2009, 1722-1729.
- van Biert, L., Godjevac, M., Visser, K. & Aravind, P. V. 2016. A review of fuel cell systems for maritime applications. *Journal of Power Sources*, 327(Supplement C), 345-364.
- Wartsila, 2016. *Wartsila 20 Project Guide* [online]. Available from: <http://cdn.wartsila.com/docs/default-source/product-files/engines/ms-engine/w%C3%A4rtsil%C3%A4-20-product-guide.pdf?sfvrsn=2> [Accessed 11th/Oct 2017].
- Welaya, Y. M. A., El Gohary, M. M. & Ammar, N. R. 2011. A comparison between fuel cells and other alternatives for marine electric power generation. *International Journal of Naval Architecture and Ocean Engineering*, 3(2), 141-149.
- Zahedi, B., Norum, L. E. & Ludvigsen, K. B. 2014. Optimized efficiency of all-electric ships by dc hybrid power systems. *Journal of Power Sources*, 255, 341-354.